Electronic Supplementary Material (ESI) for New Journal of Chemistry.

This journal is © The Royal Society of Chemistry and the Centre National de la

Recherche Scientifique 2017

Supporting Information for

Kinetics and mechanistic studies on the formation and reactivity of high valent MnO porphyrin species: mono-ortho or para-substituted porphyrins versus a di-ortho-substituted one

Rahele Nasrollahi and Saeed Zakavi*

[a] Department of Chemistry, Institute for Advanced Studies in Basic Sciences (IASBS), Zanjan 45137-66731, Iran. E-mail:zakavi@iasbs.ac.ir.

S1. ^{1}H NMR, ^{13}C NMR and UV-Vis spectral data of the porphyrins

Figure S1. UV-vis spectral changes upon the addition of TBAO to a solution of (ImH)Mn(TDClPP)(OAc) in CH_2Cl_2 (4.5×10^{-5} M, red curve, λ_{max} = 468 nm) in 1:500 ratio of TBAO (blue curve, λ_{max} = 421 and 473 nm) and also in 1:1000 ratio (orange curve, λ_{max} = 408) molar ratios.

Figure S2. UV-vis spectral changes monitored upon the oxidation of a) indene b)cyclohexene c) cyclohexen (left to right) with$[(ImH)Mn^{V}(O)(T2\text{-}Br)PP]^{+}$, $[(ImH)Mn^{V}(O)(T2\text{-}Cl)PP]^{+}$and $[(ImH)Mn^{V}(O)(T2\text{-}Br)PP]^{+}$ respectively.

Figure S3. UV-vis spectral changes monitored upon the reaction of $[(ImH)Mn^{V}(O)(TDClPP)]^{+}$($4.5 \times 10^{-5}$ M) with 4-OMestyrene (2.25×10^{-3} M). 4-Mestyrene 4-Clstyrene

Figure S4. The change in the absorbance at 407 nm vs. time for the oxidation of styrene (0.45-2.25×10^{-3} M) with $[(ImH)Mn^{V}(O)T(DCl)PP]^{+}$.

Figure S5. The change in the absorbance at 407 nm vs. time for the oxidation of 4-OMestyrene, 4-Mestyrene, 4-Clstyrene (0.45-2.25 × 10-3 M) with $(ImH)Mn^{V}(O)T(2,6\text{-}DCl)PP(OAc)$.

Scheme S1. Hydrogen bonds formed between the $Mn^{V}(O)$ porphyrins species and hydrogen bond donor molecules such as ImH and water molecules prevent the nucleophilic attack of the alkene π-orbital on the Mn=O moiety.

Figure S6. UV-vis spectral changes upon the oxidation of indene with $[(ImH)Mn^{V}(O)T(DCl)PP]^{+}$ (λ_{max} = 417 nm).

Figure S7. a) UV-vis spectrum of Mn(TPP)(OAc) (λmax = 471 nm, black curve),and (ImH)(Mn^{III}(TPP) , λ_{max} = 468 nm, red curve) and (ImH)Mn^{V}(O)(TPP) (λmax = 407 nm, blue curve) in CH_2Cl_2 b) UV-vis spectrum of Mn(TPP)(OAc) (λmax = 471 nm, black curve), and (Mn^{III}(TPP)(ImH) , λ_{max} = 468 nm, red curve) in CH_2Cl_2 and UV-vis spectral changes upon the addition of TBAO during times. (decay at 474 nm for (ImH)$Mn^{III}(OOSO_3H)$P.

Figure S8. UV-vis spectral changes monitored upon the oxidation of a) aniline b) phenyl methyl sulfide c) toluen d) cyclohexan with (ImH)Mn^{V}(O)T(2,6-DCl)PP(OAc), (ImH)Mn^{V}(O)T(2-Me)PP, (ImH)Mn^{V}(O)T(2,6-DCl)PP(OAc), (ImH)Mn^{V}(O)T(2-Me)PP(OAc) respectively.

Figure S9. The oxidation of other organic compounds, with (ImH)Mn^{V}(O)T(DCl)PP(OAc), (ImH)Mn^{V}(O)T(2-Me)PP, (ImH)Mn^{V}(O)T(DCl)PP(OAc), (ImH)Mn^{V}(O)T(2-Me)PP(OAc) respectively.

S.2 Instrumental

S.3 General oxidation procedure of alkenes

S.4 Competitive epoxidation of *cis*- and *trans*-stilbene

H_2TPP. ^{1}H NMR (400 MHz, $CDCl_3$, TMS), δ/ppm: -2.77 (2H, br, s, NH), 7.77-7.84 (8Hm and 4Hp, m), 8.26-8.27 (8Ho, d),8.90 (8Hβ, s); ^{13}C NMR (~100 MHz, $CDCl_3$, TMS), δ/ppm: 120.18 (Cmeso), 142.20 (C1), 134.60 (C2, C6), 126.73 (C3, C5),127.75 (C4), 131.5 (Cβ); UV-vis in CH_2Cl_2, λmax/nm (logε): 417 (5.79), 513 (4.58), 548 (4.38), 590 (4.30), 647 (4.29).

H_2T(4-OMe)PP. ^{1}H NMR (400MHz, $CDCl_3$, TMS), δ/ppm: -2.72 (2H, br, s, NH), 7.29-7.32 (8Hm, d), 8.15-8.17 (8Ho, d), 8.89(8Hβ, s), 4.13 (12HMe, s); ^{13}C NMR (~100MHz, $CDCl_3$, TMS), δ/ppm: 119.75 (Cmeso), 134.67 (C1), 135.62 (C2, C6), 112.20 (C3,C5), 159.39 (C4), 131.34 (Cβ), 55.61 (CMe); UV-vis in CH_2Cl_2, λmax/nm (logε)= 421 (5.61), 517 (4.32), 555 (4.22), 593 (4.06),651 (4.11).

H_2T(4-Me)PP. ^{1}H NMR (400 MHz, $CDCl_3$, TMS), δ/ppm: -2.76 (2H, br, s, NH), 7.55-7.58 (8Hm, d), 8.09-8.12 (8Ho, d), 8.86(8Hβ, s), 2.65 (12HMe, s); ^{13}C NMR (~100 MHz, $CDCl_3$, TMS), δ/ppm: 120.47 (Cmeso), 139.73 (C1), 134.92 (C2, C6), 127.81 (C3, C5), 137.71 (C4), 131.37 (Cβ), 21.57 (CMe); UV-vis in CH_2Cl_2, λmax/nm (logε): 418 (5.89), 516 (4.54), 551 (4.34), 590(4.18), 647 (4.20).

H_2T(2-Me)PP. ^{1}H NMR (400 MHz, $CDCl_3$, TMS), δ/ppm: -2.59 (2H, br, s, NH), 7.54-7.74 (8Hm and 4Hp, m, meta and paraposition relative to C atom attached to meso position), 7.99-8.11 (4Ho, m, ortho-position relative to C atom attached to meso position), 8.70 (8Hβ, s), 2.01-2.11 (12HMe, m);); ^{13}C NMR (~100 MHz, $CDCl_3$, TMS), δ/ppm: 118.82 (Cmeso), 139.54 (C1),139.63 (C2), 128.38 (C3), 129.22 (C4), 124.21 (C5), 133.90 (C6), 141.48 (Cα), 129.22 (Cβ), 21.37 (CMe); UV-vis in CH_2Cl_2,λmax/nm (logε): 416 (6.04), 512 (4.74), 545 (4.34), 589 (4.34), 645 (4.25).

H_2T(2-Cl)PP. ^{1}H NMR (400MHz, $CDCl_3$, TMS), δ/ppm: -2.62 (2H, br, s, NH), 7.66-7.87 (8Hm and 4Hp, m, meta and paraposition relative to C atom attached to meso position), 8.10-8.26 (4Ho, m, ortho-position relative to C atom attached to mesoposition), 8.72 (8Hβ, s); ^{13}C NMR (~100 MHz, $CDCl_3$, TMS), δ/ppm: 116.76 (Cmeso), 137.10 (C1), 136.94 (C2), 129.01 (C3),129.93 (C4), 125.32 (C5), 135.52 (C6), 140.50 (Cα), 135.39 (Cβ); UV-vis in CH_2Cl_2, λmax/nm (logε): 416 (5.64), 512 (4.47), 543(4.07), 587 (4.15), 643 (3.96).

H_2T(2-Br)PP. ^{1}H NMR (400MHz, $CDCl_3$, TMS), δ/ppm: -2.6 (2H, br, s, NH), 7.67-7.76 (8Hm and 4Hp, m, meta and paraposition relative to C atom attached to meso position), 8.03-8.08 (4Ho, m, ortho-position relative to C atom attached to mesoposition), 8.71 (8Hβ, s); ^{13}C NMR (~100 MHz, $CDCl_3$, TMS), δ/ppm: 118.60 (Cmeso), 142.50 (C1), 127.41 (C2), 130.03 (C3),127.57 (C4), 125.85 (C5), 135.27 (C6), 145.53 (Cα), 132.03 (Cβ).

H_2T(4-Cl)PP. ^{1}H NMR (400 MHz, $CDCl_3$, TMS), δ/ppm: -2.83 (2H, br, s, NH), 7.77-7.79 (8Hm, d), 8.15-8.17 (8Ho, d), 8.87(8Hβ, s); ^{13}C NMR (~100 MHz, $CDCl_3$, TMS), δ/ppm: 119.01 (Cmeso), 140.37 (C1), 135.52 (C2, C6), 127.07 (C3, C5), 134.41(C4), 131.64 (Cβ); UV-vis in CH_2Cl_2, λmax/nm (logε): 418 (5.79), 513 (4.52), 547 (4.25), 590 (4.16), 647 (4.10).

H_2T(2-NO_2)PP. ^{1}H NMR (400 MHz, DMSO-d6, TMS), δ/ppm: - 2.83 (s, 2H, NH), 8.61 (s, 8H, Hβ), 8.30 (m, 4H, Ho), 8.45 (m,8H, Hm), 7.98 (m, 4H, Hp); UV-vis in CH_2Cl_2, λmax/nm (logε): (See ESI,† S3-1).

H_2T(2,6-Cl)PP. ^{1}H NMR (400 MHz, $CDCl_3$, TMS), δ/ppm: -2.59 (2H, br, s, NH), 7.68 (12H, m, Hm,p), 8.66 (8H, s, Hβ,); UVvis in CH_2Cl_2, λmax/nm (logε): (See ESI,† S3-1).

H_2T(4-py)PP. ^{1}H NMR (400 MHz $CDCl_3$,):δ/ppm-2.93 (2H, br, s, NH),8.15–8.17 (8Hm, dd), 9.06–9.07 (8Ho, dd), 7.90 (4H, m), 8.87 (8H,s); UV–Vis (/nm) in CH_2Cl_2: 418 (Soret), 512, 547, 588, 646.

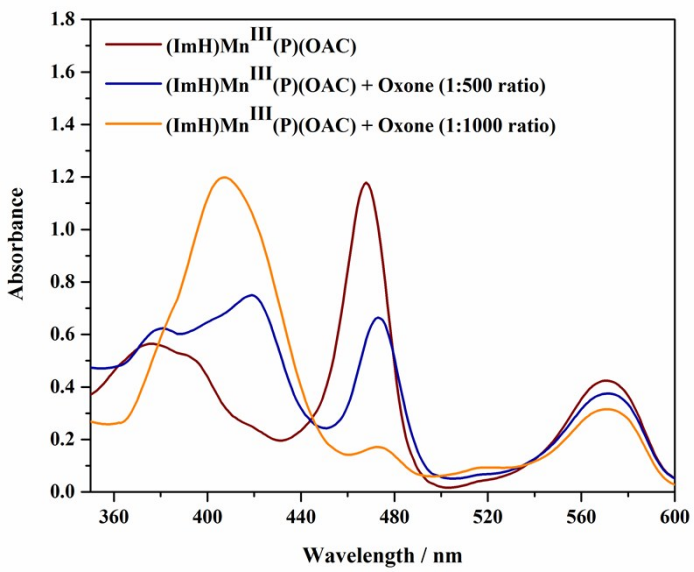

Figure S1. UV-vis spectral changes upon the addition of TBAO to a solution of (ImH)Mn(TDClPP)(OAc) in CH_2Cl_2 (4.5×10^{-5} M, red curve, λ_{max} = 468 nm) in 1:500 ratio of TBAO (blue curve, λ_{max} = 421 and 473 nm) and also in 1:1000 ratio (orange curve, λ_{max} = 408) molar ratios.

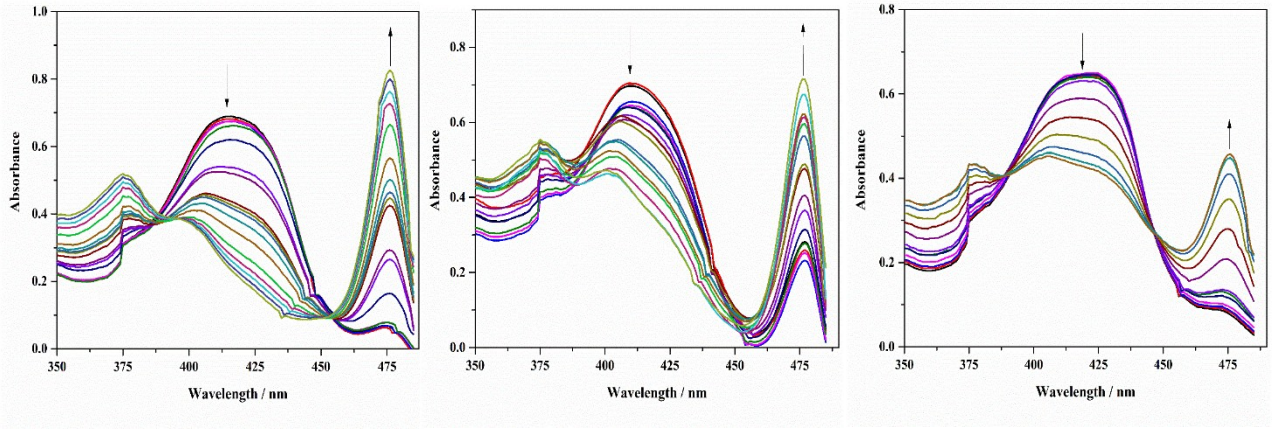

Figure S2. UV-vis spectral changes monitored upon the oxidation of a) indene b)cyclohexene c) cyclohexen (left to right) with[(ImH)Mn^{V}(O)(T2-Br)PP]$^{+}$, [(ImH)Mn^{V}(O)(T2-Cl)PP]$^{+}$and [(ImH)Mn^{V}(O)(T2-Br)PP]$^{+}$ respectively.

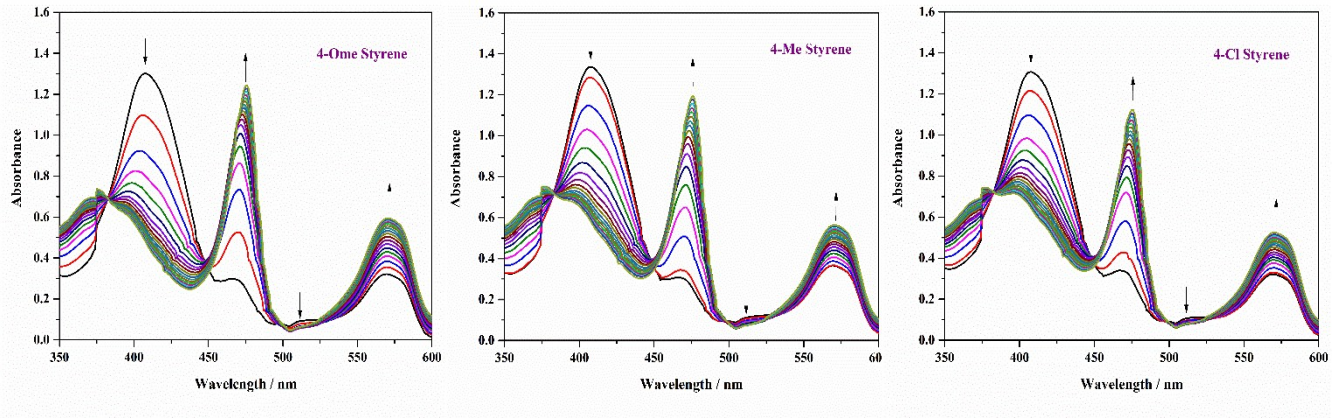

Figure S3. UV-vis spectral changes monitored upon the reaction of $[(ImH)Mn^{V}(O)(TDClPP)]^{+}$(4.5 × 10^{-5} M) with 4-OMestyrene (2.25 × 10^{-3} M). 4-Mestyrene 4-Clstyrene

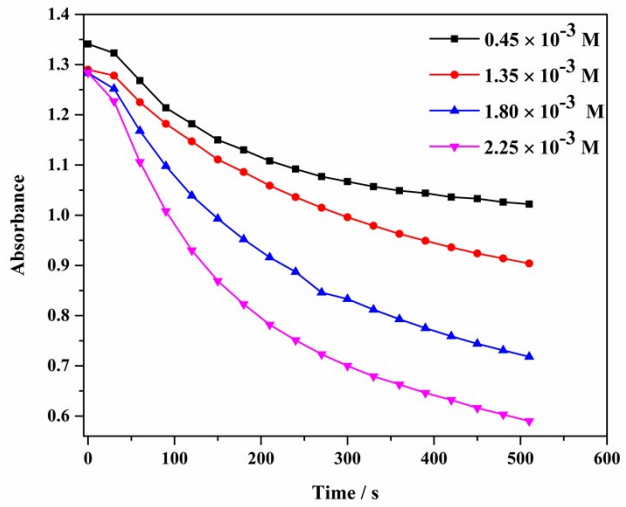

Figure S4. The change in the absorbance at 407 nm vs. time for the oxidation of styrene (0.45-2.25 × 10^{-3} M) with $[(ImH)Mn^{V}(O)T(DCl)PP]^{+}$

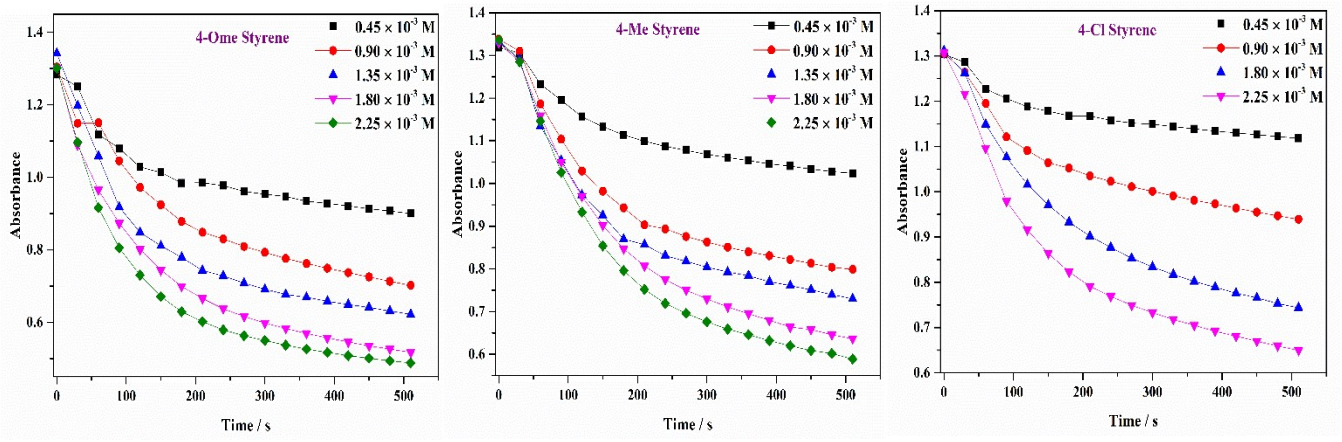

Figure S5. The change in the absorbance at 407 nm vs. time for the oxidation of 4-OMestyrene, 4-Mestyrene, 4-Clstyrene (0.45-2.25 × 10-3 M) with (ImH)Mn^{V}(O)T(2,6-DCl)PP(OAc).

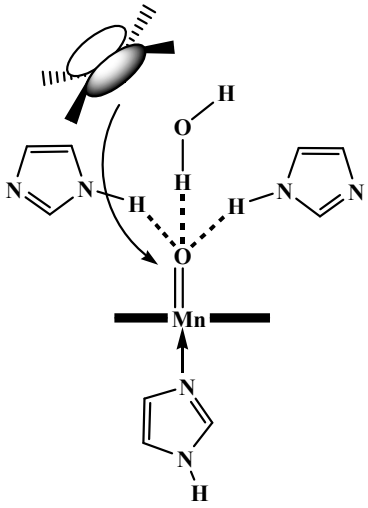

Scheme S1. Hydrogen bonds formed between the Mn^{V}(O) porphyrins species and hydrogen bond donor molecules such as ImH and water molecules prevent the nucleophilic attack of the alkene π-orbital on the Mn=O moiety.

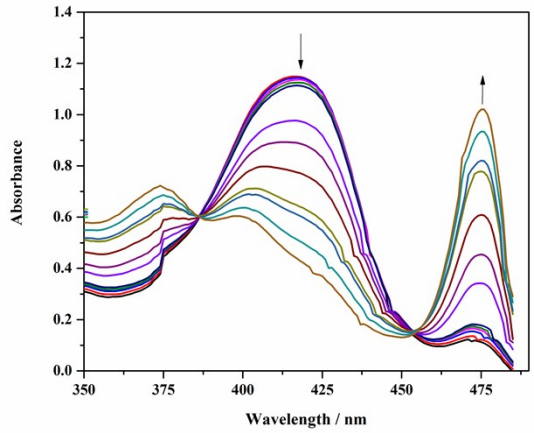

Figure S6. UV-vis spectral changes upon the oxidation of indene with $[(ImH)Mn^{V}(O)T(DCl)PP]^{+}$ (λ_{max} = 417 nm).

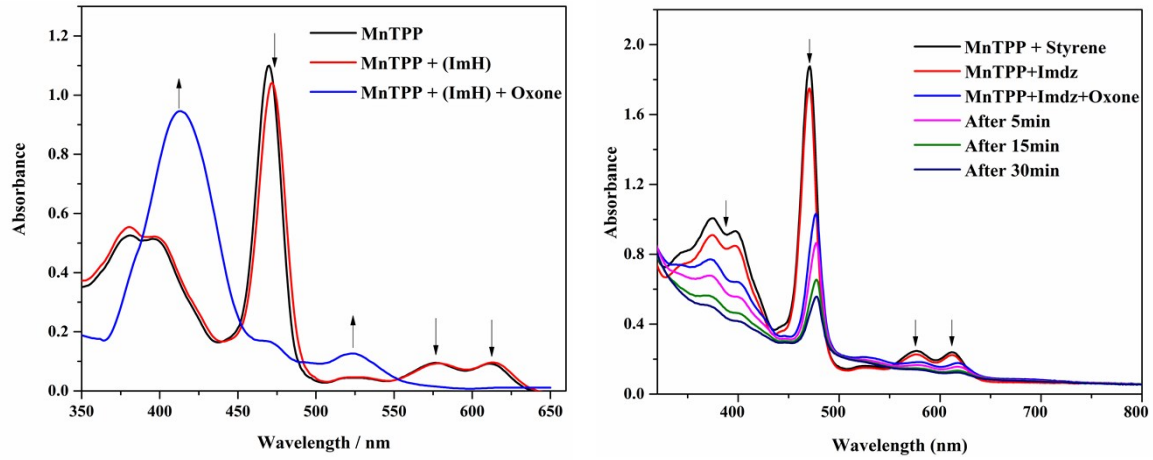

Figure S7. a) UV-vis spectrum of Mn(TPP)(OAc) (λ_{max} = 471 nm, black curve), and $(ImH)(Mn^{III}(TPP)$, λ_{max} = 468 nm, red curve) and $(ImH)Mn^{V}(O)(TPP)$ (λ_{max} = 407 nm, blue curve) in CH_2Cl_2 b) UV-vis spectrum of Mn(TPP)(OAc) (λ_{max} = 471 nm, black curve), and $(Mn^{III}(TPP)(ImH)$, λ_{max} = 468 nm, red curve) in CH_2Cl_2 and UV-vis spectral changes upon the addition of TBAO during times. (decay at 474 nm for $(ImH)Mn^{III}(OOSO_3H)P$.

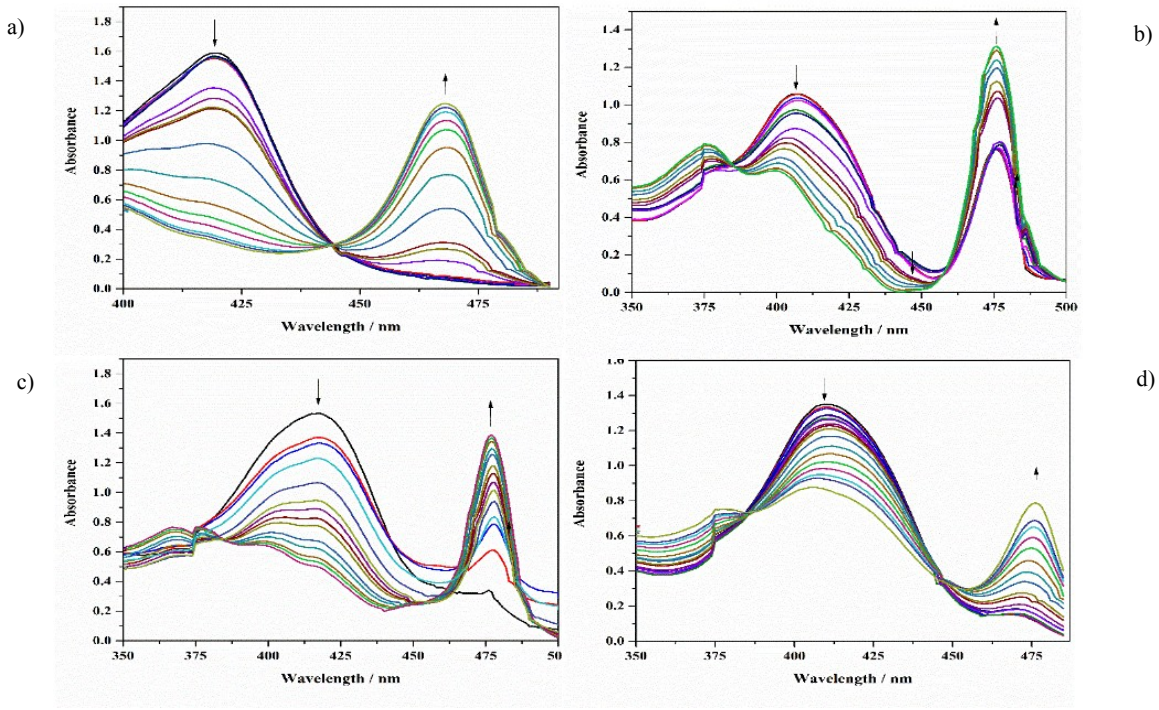

Figure S8. UV-vis spectral changes monitored upon the oxidation of a) aniline b) phenyl methyl sulfide c) toluen d) cyclohexan with (ImH)Mn^{V}(O)T(2,6-DCl)PP(OAc), (ImH)Mn^{V}(O)T(2-Me)PP, (ImH)Mn^{V}(O)T(2,6-DCl)PP(OAc), (ImH)Mn^{V}(O)T(2-Me)PP(OAc) respectively.

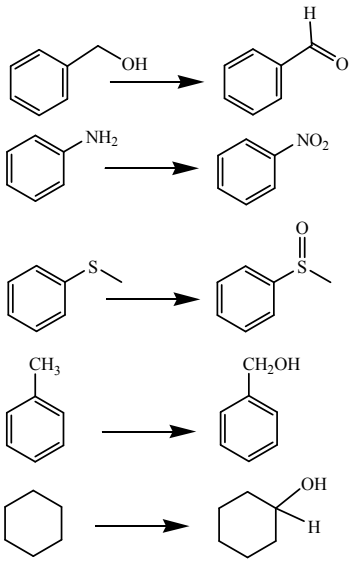

Figure S9. The oxidation of other organic compounds, with (ImH)Mn^{V}(O)T(DCl)PP(OAc), (ImH)Mn^{V}(O)T(2-Me)PP, (ImH)Mn^{V}(O)T(DCl)PP(OAc), (ImH)Mn^{V}(O)T(2-Me)PP(OAc) respectively (see also Figure S8).

S.2 Instrumental

UV−vis spectral studies were carried out using a Pharmacia Biotech Ultrospec 4000 UV–Vis spectrophotometer. ^{1}H NMR spectra were obtained on a BrukerAvance DPX-400 MHz spectrometer. The reaction products were analyzed by a Varian-3800 gas chromatograph equipped with a HP-5 capillary column and flame-ionization detector using authentic samples to identify the oxidation products.

S.3 General oxidation procedure of alkenes

In a typical reaction, ImH (4.5×10^{-4} M in CH_2Cl_2) was added to the solution of Mn-porphyrins (4.5×10^{-5} M) to achieve the desired molar ratio of catalyst to ImH (1:15). The solution was stirred for 5 min before the addition of oxidant. TBAO (4.5×10^{-2} M) was added to this solution until all of MnT(DCl)PP(OAc) was converted to Mn^{V}(O); the formation of the high valentMn(O) species completed at 1:1000 molar ratio of catalyst to TBAO. The oxidation reaction was conducted by addition of excess amounts of the organic substrate to meet pseudo-first order conditions (0.45×10^{-3} M to 2.25×10^{-3} M). The observed rate constants (k_{obs}) have been determined using different concentrations of substrate and a nonlinear curve fitting [$A_t = A_f + (A_0 - A_f)\exp(-k_{obs}t)$]. Each experiment was triplicated. All experiments were carried out in CH_2Cl_2 and a 1.0 cm glass cell at 273 K. The progress of reaction was monitored by measuring the change in the absorbance at 407, and 474 nm. The reaction products were analyzed by GC. Also, control reactions conducted in CCl_4 were utilized to characterize the product directly by ^{1}H NMR. The oxidation of styrenes, cyclohexene and indene gave the corresponding epoxide as the sole product.

S.4 Competitive epoxidation of *cis*- and *trans*-stilbene

For the competitive oxidation of stilbenes, MnT(DCl)PP (OAc), ImH, (*cis*- and *trans*-stilbene) and TBAO were used in 1:15:(500,500):1000 molar ratio. In a typical reaction, MnT(DCl)PP(OAc) (7.5×10^{-4} mmol), ImH (1.125×10^{-2}mmol)*cis*-stilbene (0.375 mmol), *trans*-stilbene (0.375mmol) and TBAO (7.5×10^{-2}mmol) were added to a 5 ml round bottom flask containing 2 ml CCl_4 and magnetically stirred for 30 min. The reaction mixture was directly analyzed by ^{1}H NMR to determine the cis- to trans oxide molar ratio. Also, the reaction was conducted using the 1:15:(500,500):200 molar ratio using 7.5×10^{-4} mmol MnT(DCl)PP(OAc), 1.125×10^{-2}mmolImH, 0.375mmolstilbenes and 1.5×10^{-2} mmol TBAO.